IOP Publishing *New J. Phys.* **00** (2015) 000000

New Journal of Physics
The open access journal at the forefront of physics

Deutsche Physikalische Gesellschaft DPG
IOP Institute of Physics

Published in partnership with: Deutsche Physikalische Gesellschaft and the Institute of Physics

PAPER

Collisional relaxation of vibrational states of SrOH with He at 2 K

Ivan Kozyryev[1,2], **Louis Baum**[1,2], **Kyle Matsuda**[1,2], **Peter Olson**[1], **Boerge Hemmerling**[1,2] **and John M Doyle**[1,2]

[1] Harvard-MIT Center for Ultracold Atoms, Cambridge, MA 02138, USA
[2] Department of Physics, Harvard University, Cambridge, MA 02138, USA

Keywords: buffer-gas cooling, vibrational quenching, cold polyatomic molecules

Supplementary material for this article is available online

OPEN ACCESS

RECEIVED
11 January 2015

REVISED
17 February 2015

ACCEPTED FOR PUBLICATION
4 March 2015

PUBLISHED
DD MM 2015

Abstract

Vibrational relaxation of strontium monohydroxide (SrOH) molecules in collisions with helium (He) at 2 K is studied. We find the diffusion cross section of SrOH at 2.2 K to be $\sigma_d = (5 \pm 2) \times 10^{-14}$ cm^2 and the vibrational quenching cross section for the (100) Sr–O stretching mode to be $\sigma_q = (7 \pm 2) \times 10^{-17}$cm^2. The resulting ratio $\gamma_{100} = \sigma_d/\sigma_q \sim 700$ is more than an order of magnitude smaller than for previously studied few-atom radicals (Au *et al* 2014 *Phys. Rev.* A 90 032703). We also determine the Franck–Condon factor for SrOH ($\tilde{A}^2\Pi_{1/2}(100) \leftarrow \tilde{X}^2\Sigma^+(000)$) to be $(4.8 \pm 0.8) \times 10^{-2}$.

1. Introduction

The study and control of cold atom–molecule collisions lies at the interface of physics and chemistry [1–3]. The diversity and complexity of internal molecular structures and molecular interactions provide new possibilities in precision measurement [4, 5], quantum information science [6, 7], condensed-matter physics [8], and controlled chemistry [3]. Detailed understanding of low temperature molecular collisions provides important information necessary for further development of these applications.

Compared to atomic collisions [9], low-temperature collisions of diatomic molecules are much less understood. Recently, however, significant progress has been made [10–12]. Experimental measurements of low energy collisions between simple polyatomic species (like linear triatomics) and atoms can provide crucial input for advancing theoretical models. Supersonic jet beams (sometimes Stark decelerated [13, 14]), atom association [15–17], and buffer-gas cooling [18–20] are the main experimental tools for exploring molecular collisions in the cold (1 K) and ultracold (1 μK) temperature regimes. The cold, rarefied buffer-gas environment offers a way to study cooling and molecular collisions with precise control of helium buffer-gas density and cell temperature. The efficiency of quenching vibrational motion during the atom–molecule collisional process at low temperature has been recently measured for several systems [21–24].

In this paper, we explore inelastic collisions between strontium monohydroxide (SrOH) and helium (^{4}He) at 2.2 K. Our measurements probe the intermediate range of vibrational energy spacings, compared to previous low temperature collisional results [22–25]. For the excited Sr–O stretching vibrational mode of SrOH, we observe rapid rotational quenching and translational cooling followed by a slower vibrational quenching to the ground vibrational level. Vibrational quenching cross sections are determined with high accuracy. Our work extends the study of vibrational relaxation in cold atom–molecule collisions to linear polyatomic radicals and contributes to an overall physical picture of the dependence of quenching rates on vibrational energy spacing in low energy collisions, providing an important benchmark for theory.

2. Experiment

To create cold SrOH molecules we use laser ablation in combination with buffer-gas cooling [26]. A schematic diagram of the experimental apparatus is shown in figure 1. SrOH ($\tilde{X}^2\Sigma^+$) molecules are introduced into the gas

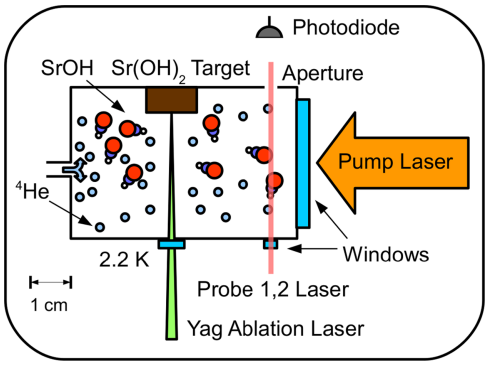

Figure 1. Schematic of the apparatus. Hot SrOH molecules produced during laser ablation of a $Sr(OH)_2$ target quickly cool translationally and rotationally after colliding with cold (~2 K) helium buffer gas. Thermalization dynamics are studied using a probe laser to observe molecular absorption. An optical pumping beam is used to populate $\tilde{X}$ (100) vibrational level to measure the quenching rate.

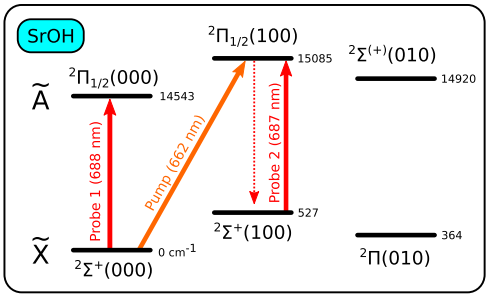

Figure 2. Optical pumping and detection procedure for SrOH. The energies are specified in cm^{-1} and taken from [28]. The vibrational quantum numbers (*nml*) correspond to the Sr ↔ OH stretching mode (*n*), the Sr–O–H bending mode (*m*) and the SrO↔H stretching mode (*l*). Rotational states are not shown at this scale. Excitation lasers are shown with solid lines. Spontaneous emission is depicted with a dashed line.

phase using pulsed Nd:YAG laser ablation at 532 nm of a $Sr(OH)_2$ solid precursor with a pulse energy of ~15 mJ and duration of ~5 ns. We continuously flow ^{4}He buffer gas into a 2.5 cm-diameter cell at rates of 0.5–10 standard cubic centimeters per minute (SCCM). The cell is thermally anchored to a pumped helium reservoir at a temperature of $T \sim 2.2$ K. The helium density in a cell can be varied between $n_{He} \approx 1 \times 10^{15} - 1 \times 10^{16}$ cm^{-3}, resulting in the typical mean time between molecule-helium diffusive collisions of $\tau \sim 0.6 - 0.06$ μs. The typical SrOH density in our experiment is a very small fraction of the helium density $n_{SrOH} \approx 10^9$ cm^{-3}. A detailed description of the cryogenic apparatus used in this experiment is provided by [27].

Laser absorption spectroscopy is performed in the cell to monitor molecule production and thermalization dynamics. SrOH in the ground and excited vibrational levels is detected using 'diagonal' $\tilde{A}^2\Pi_{1/2} \leftrightarrow \tilde{X}^2\Sigma^+$ transitions. We use external-cavity diode lasers at 688 nm with a typical detection power of $P \sim 5$ μW and a beam diameter of ø ~ 1 mm. We employ the 'off-diagonal' excitation $\tilde{A}^2\Pi_{1/2}(100) \leftarrow \tilde{X}^2\Sigma^+(000)$ at 662 nm (25 mW for ø ~ 2 cm) followed by $\tilde{A}^2\Pi_{1/2}(100) \rightarrow \tilde{X}^2\Sigma^+(100)$ spontaneous emission ($\tau_{sp} \approx 30$ ns) for optical pumping of ground state molecules into $\tilde{X}(100)$ state. The relevant energy levels and lasers are shown in figure 2. We use a mechanical shutter to block the optical pumping beam with a closing time $t \leqslant 150$ μs.

3. Results and discussion

3.1. SrOH–He diffusion cross section

We determine the SrOH–He diffusion cross section by measuring the time dynamics in the buffer-gas cell of molecules in the $\tilde{X}^2\Sigma^+(000)$, $N = 1$ state, which is the most populated rotational level at 2 K (figure 8). The spectrum of the ground vibrational level of cold SrOH in the first excited rotational level ($N = 1$) is shown in figure 3. The time decay profile of the molecules in the $\tilde{X}(000)$ vibronic state is governed by the diffusion to the walls and pump-out of the cell through the aperture:

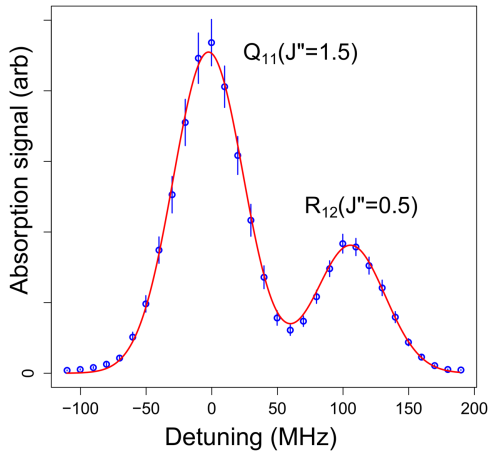

Figure 3. Spectrum of cold gas-phase SrOH molecules in the $\tilde{X}^2\Sigma^+(000)$ vibronic, first excited rotational ($N=1$) state using $\tilde{A}^2\Pi_{1/2} \leftarrow \tilde{X}^2\Sigma^+$ electronic transition ~5 ms after laser ablation. The two measured peaks are for different spin-rotation components in the electronic ground state ($J'' = 0.5$ and 1.5) of the $N=1$ level. We perform a Doppler fit of the form $y = a \cdot e^{-(x-b)^2/\gamma_D^2}$ to each resonance line separately. Measured Doppler width $\gamma_D \approx 38 \pm 1$ MHz corresponds to a translational temperature of 4.3 ± 0.1 K.

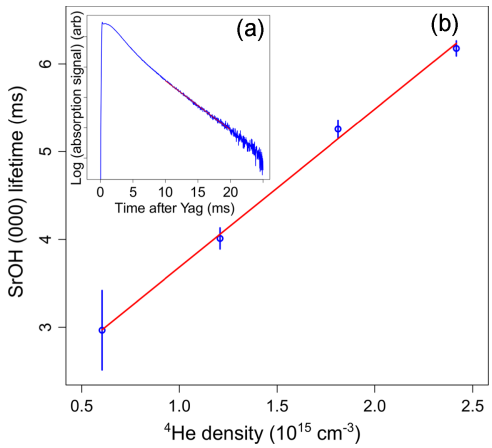

Figure 4. (a) Time decay of SrOH molecules in the (000) vibrational mode at the buffer-gas flow of 2 sccm with the linear fit shown. (b) In-cell lifetime for the ground vibronic, first excited rotational ($N=1$) level of SrOH for various buffer-gas densities with a linear fit. For low buffer-gas flows (shown here) the molecule loss is dominated by diffusion to the cell walls.

$$\frac{1}{\tau_{000}} = \frac{1}{\tau_d} + \frac{1}{\tau_p}, \tag{1}$$

where τ_{000}, τ_d, and τ_p are the timescales for the decay of (000) vibrational mode molecules (τ_{000}) due to diffusion (τ_d) and cell pump-out (τ_p). By measuring the on-resonance absorption time profile (figure 4(a)) we can extract the diffusion lifetime of SrOH: $\tau_d = \left(1/\tau_{000} - 1/\tau_p\right)^{-1}$. For low buffer-gas flows $\tau_d/\tau_p < 1$ [29], and the molecule loss is primarily due to diffusion to the cell walls. Therefore, from our measurements of τ_{000} we can directly determine the diffusion lifetime of the molecules in our cell: $\tau_d \approx \tau_{000}$.

At long times after laser ablation ($\gtrsim$10 ms), when higher-order diffusion modes have decayed, the in-cell $\tilde{X}(000)$ population profile is well fitted by a single exponential (figure 4(a)). We determine the SrOH–He momentum transfer cross section by measuring the diffusion lifetime of SrOH (000) mode molecules at different densities of helium buffer gas. From figure 4(b) we find that τ_{000} has a linear dependance on the helium density and conclude that (000) mode molecule loss is primarily dominated by diffusion. For a cylindrical cell of length L and radius r the time constant of the exponential decay for molecules diffusing through helium gas of density (n_{He}) is given by [30]:

$$\tau_d = \frac{n_{He}\sigma_d}{\bar{\nu}G}, \tag{2}$$

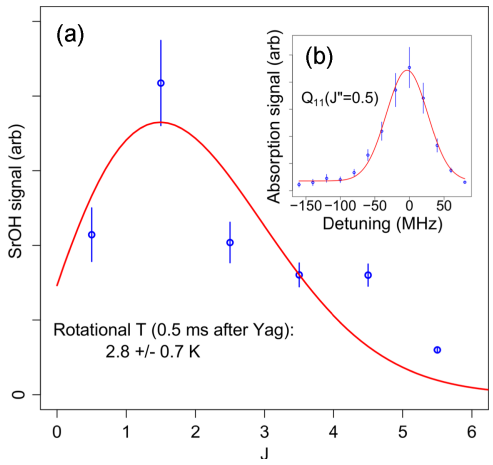

Figure 5. (a) Rotational state $(N = J - 1/2)$ population for SrOH $\tilde{X}^2\Sigma^+(100)$ vibrational mode 500 μs after laser ablation. The measurement was performed using $Q_{11}(J'')$ line absorption on the $\tilde{A}^2\Pi_{1/2}(100) \leftarrow \tilde{X}^2\Sigma^+(100)$ electronic transition. From the Boltzmann distribution fit, we conclude that molecules in the excited vibrational level quickly thermalize rotationally to the cell temperature of ~2 K. (b) Spectrum of cold gas-phase SrOH molecules in the $\tilde{X}^2\Sigma^+(100)$ vibronic, ground rotational $(N=0)$ state using $\tilde{A}^2\Pi_{1/2} \leftarrow \tilde{X}^2\Sigma^+$ electronic transition ~0.5 ms after laser ablation. We perform a Doppler fit of the form $y = a \cdot e^{-(x-b)^2/\gamma_D^2}$ to obtain a Doppler width $\gamma_D \approx 42 \pm 2$ MHz, corresponding to a translational temperature of 5.3 ± 0.3 K.

$$G = \frac{3\pi}{32}\left(\frac{j_{01}^2}{r^2} + \frac{\pi^2}{L^2}\right), \tag{3}$$

where $\bar{v} = \left(8k_B T/\pi\mu\right)^{1/2}$ is the mean SrOH–^{4}He collision velocity at temperature T with reduced mass of the atom–molecule system μ and the diffusion cross section σ_d ($j_{01} \approx 2.405$ is the first root of the Bessel function $J_0(x)$). From equation (2) we determine that in the diffusive regime $(\tau_d/\tau_p < 1)$ the in-cell lifetime is directly proportional to the helium density, as seen in our data.

From the measurement of τ_{000} as a function of the helium density (figure 4(b)) using equation (2) we can extract the value of the diffusion cross section, $\sigma_d \approx \tau_{000}\bar{v}G/n_{He}$, finding the SrOH diffusion cross section in He at 2.2 K to be $\sigma_d\left(\text{SrOH} - {}^4\text{He}\right) = (5 \pm 2) \times 10^{-14}$ cm^2. The measured SrOH–He diffusion cross section is somewhat larger than previously measured for diatomic molecules [19, 25] at similar temperatures. The measured value of $\sigma_d\left(\text{SrOH} - {}^4\text{He}\right)$ agrees with the theoretical prediction for larger polyatomic molecules colliding with helium [31].

3.2. Vibrational quenching cross sections

Vibrationally excited SrOH molecules are produced during the process of laser ablation. As can be seen from figure 5, vibrationally excited molecules of the (100) Sr–O stretching mode quickly (<500 μs) thermalize rotationally to $T_r = 2.8 \pm 0.7$ K and translationally to a temperature ⩽5.6 K. We place a bound on the translational temperature from the Doppler fit. Additional linewidth broadening mechanisms are present inside buffer-gas cells as has been seen repeatedly [25]. Vibrational temperature remains out of thermal equilibrium ($T_v \sim 400$ K) with other degrees of freedom.

In order to populate $\tilde{X}(100)$ state we optically pump SrOH molecules from the (000) mode to the (100) mode using $\tilde{A}^2\Pi_{1/2}(100) \leftarrow \tilde{X}^2\Sigma^+(000)$ electronic excitation (figure 2). Optical pumping process increases the population in $\tilde{X}(100)$ state by an order of magnitude. After the optical pumping laser is turned off, SrOH molecules in the (100) mode decay faster than those in the (000) mode (figure 6). The additional effect that leads to the faster decay for the (100) molecules is vibrational quenching with timescale τ_q. Using equation (1), we can write the decay rate of the (100) molecules in the buffer-gas cell:

$$\frac{1}{\tau_{100}} = \frac{1}{\tau_q} + \frac{1}{\tau_d} + \frac{1}{\tau_p}. \tag{4}$$

In the regime where vibrational quenching dominates other loss processes $(\tau_q < \tau_d, \tau_p)$, the measurement of the (100) lifetime gives quenching time: $\tau_{100} \approx \tau_q = \left(\Gamma_q n_{He}\right)^{-1}$. As can be seen from figure 7(a), the in-cell lifetime of the molecules in the $\tilde{X}(100)$, $N = 1$ state is inversely proportional to the helium density which indicates that (100) molecule loss is dominated by vibrational quenching.

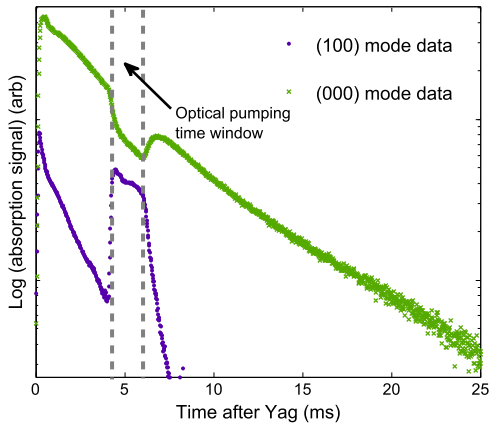

Figure 6. SrOH absorption signal versus time for different vibrational modes: vibrational ground state (000) and Sr–O stretching mode (100). The optical pumping laser excites molecules from the $\tilde{X}^2\Sigma^+(000)$ state to $\tilde{A}^2\Pi_{1/2}(100)$ state on $Q_{11}(J'' = 1.5)$ transition. Excited molecules predominantly decay to $\tilde{X}^2\Sigma^+(100)$ state. After the optical pumping laser is turned off, the decay of molecules in the (100) mode is dominated by vibrational quenching. We monitor populations in the different modes using $Q_{11}(J'' = 1.5)$ bands of the $\tilde{A}^2\Pi_{1/2} \leftarrow \tilde{X}^2\Sigma^+$ electronic transitions.

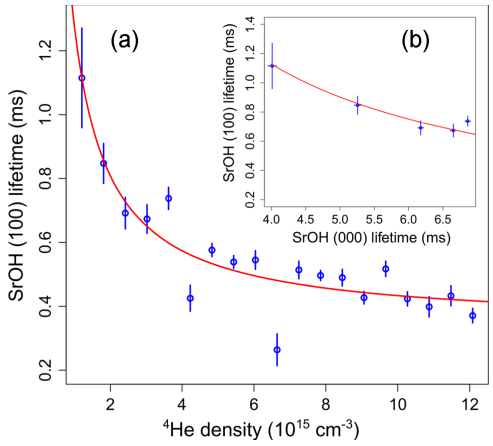

Figure 7. (a) Observed vibrational quenching for $\tilde{X}^2\Sigma^+(100)$, $N = 1$ state of SrOH in collisions with ^{4}He at 2 K. Helium flow is proportional to the in-cell buffer gas density. (b) The plot of (100) mode lifetime against (000) mode lifetime for a range of in-cell helium densities. The fit is to the expected functional form $\tau_{100} \propto \Gamma/\tau_{000}$.

The dimensionless ratio of elastic to inelastic collision rates γ_{100} indicates the rate of translational versus vibrational equilibration of a molecular sample and can be determined from our measurements by:

$$\gamma_{100} = \frac{\Gamma_\mathrm{d}}{\Gamma_\mathrm{q}} = \frac{\sigma_\mathrm{d}\bar{v}}{(\tau_\mathrm{q} n_\mathrm{He})^{-1}} = \bar{v}^2 G \tau_\mathrm{d} \tau_\mathrm{q}, \tag{5}$$

where we used equation (2) in the last step. After extracting lifetimes for the decays of the (000) and (100) vibrational modes (figure 7(b)), we calculate γ_{100} using an approximate form of equation (5):

$$\gamma_{100} \approx \bar{v}^2 G \tau_{000} \tau_{100} \tag{6}$$

at various buffer-gas densities. The measured value for SrOH(100)–^{4}He collisions is $\gamma_{100} = 680 \pm 80$ at 2.2 K, i.e. SrOH $\tilde{X}(100)$ molecules undergo approximately 700 momentum changing collisions before quenching vibrationally.

We can also place an upper bound on γ_{010} for the excited bending mode. The number of collisions necessary for translational cooling of vibrationally excited SrOH molecules produced during laser ablation is given by [32]:

$$N = -\kappa \ln\left[\frac{T_f - T_\mathrm{bg}}{T_i}\right] \approx 100 \tag{7}$$

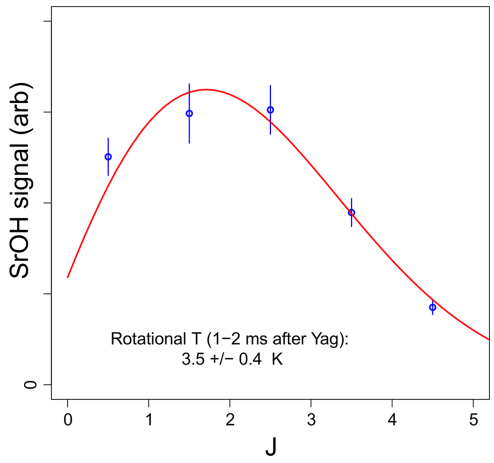

Figure 8. Thermal distribution of rotational levels $(N = J - 1/2)$ for the ground vibrational mode (000) of SrOH 1–2 ms after laser ablation. From the Boltzmann distribution fit $y = a\,(2J+1)\,e^{-BJ\,(J+1)/T}$ ($B_{\mathrm{SrOH}} = 0.36$ K), we obtain the rotational temperature $T = 3.5 \pm 0.4$ K.

for $T_f = 4$ K, $T_{\mathrm{bg}} = 2$ K and the coefficient $\kappa \equiv \left(m_{\mathrm{SrOH}} + m_{\mathrm{He}}\right)^2 \Big/ \left(2m_{\mathrm{SrOH}}\, m_{\mathrm{He}}\right)$. Therefore, if $\gamma > 100$, the sample will cool translationally and rotationally, before collision-induced vibrational relaxation, leaving a metastable population, as was seen in the (100) mode of SrOH. However, if $\gamma < 100$ vibrationally excited molecules will quench before they cool translationally and rotationally. Molecules in the $\tilde{X}^2\Pi\,(010)$ vibronic state were previously detected in supersonic beams for SrOH [33] and CaOH [34] produced using pulsed laser ablation at 300 K. Experimentally, when measuring absorption on $\tilde{A}^2\Sigma^{(+)}(010) \leftarrow \tilde{X}^2\Pi\,(010)$ band we saw no evidence of molecules in the excited bending mode. This rapid vibrational thermalization is due to inelastic vibrational collisions with helium. This allows us to place an upper bound $\gamma_{010} < 100$, which is consistent with direct experimental measurements for low-lying bending modes in large molecules [24]. In addition to vibrational quenching, there could potentially be other unexpected contributions to the loss of (010) molecules in our experiment like state dependent chemical reactions.

The measured values of γ can be used to calculate the absolute values of collisional quenching cross sections:

$$\sigma_{\mathrm{q}} = \sigma_{\mathrm{d}}/\gamma. \tag{8}$$

Combining our measurements of γ and σ_{d} we obtain the following values for the vibrational quenching cross sections $\sigma_{\mathrm{q}}(100) = (7 \pm 2) \times 10^{-17}$ cm^2 and $\sigma_{\mathrm{q}}(010) > 5 \times 10^{-16}$ cm^2.

3.3. Rotational thermalization

Rotational thermalization dynamics for SrOH molecules in (100) and (000) vibrational modes can be extracted by monitoring $Q_{11}(J'')$ transitions for different rotational levels. From the data shown in figures 5 and 8, we estimate that rotational temperature thermalizes to $T_{\mathrm{r}} \sim 3$ K within 1 ms after ablation. Since the mean time between collisions is <1 μs we conclude that fewer than 1000 collisions are necessary for complete rotational thermalization after laser ablation. The initial rotational temperature following laser ablation process in a similar experiment was measured to be >300 K [35]. Typically, initial translational temperature of species immediately after the ablation process is ~1000 K [26, 36].

3.4. Franck–Condon (FC) factor measurements

Diagonal FC factors are required for scattering thousands of photons necessary for laser cooling or slowing of molecules [37]. Experimental measurements of these factors have focused on diatomic molecules thus far [38–40]. We measure the ratio of FC factors by comparing the ratio of the absorption signals R_{sig} for $\tilde{A}^2\Pi_{1/2}(100) \leftarrow \tilde{X}^2\Sigma^+(000)$ and $\tilde{A}^2\Pi_{1/2}(000) \leftarrow \tilde{X}^2\Sigma^+(000)$ transitions using $Q_{11}(J'' = 1.5)$ lines shown in figure 9(b). Since the absorption cross section σ for a Doppler broadened line in an electronic transition is proportional to the product of the excitation frequency (ν) and FC factor ($q_{v'-v''}$) as $\sigma \propto \nu q_{v'-v''}$ [41, 42], the ratio of FC factors from our measurements is given by:

$$R_{\mathrm{FC}} = \frac{\nu_{000\leftarrow 000}}{\nu_{100\leftarrow 000}} \times R_{\mathrm{sig}}, \tag{9}$$

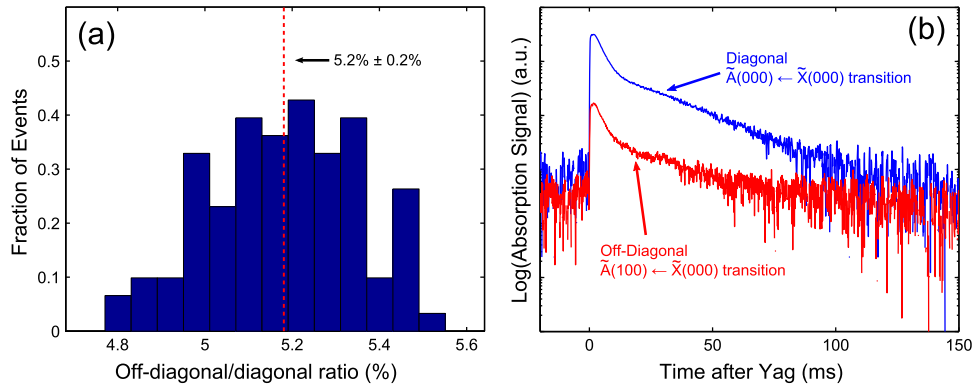

Figure 9. (a) Histogram of the ratio of the absorption signals for the $Q_{11}(J'' = 1.5)$ resonant lines in SrOH exiting the diagonal $\tilde{A}^2\Pi_{1/2}(000) \leftarrow \tilde{X}^2\Sigma^+(000)$ and off-diagonal $\tilde{A}^2\Pi_{1/2}(100) \leftarrow \tilde{X}^2\Sigma^+(000)$ electronic transitions. We observe an average value of 5.2% with a standard deviation of 0.2%. Figure (b) shows the corresponding absorption signals as a function of time. To determine the histogram of the measured ratios, only the signal between 0.5 and 10 ms is used in the analysis.

where R_{sig} is the ratio of the absorption signals and ν is the frequency of the corresponding transition. The Born–Oppenheimer approximation and the FC separation of electronic and vibrational motions was applied to the Sr–O stretching mode in the $\tilde{A}$ state of SrOH [41, 43]. We obtain $R_{sig} = 5.2 \pm 0.2\%$ which gives $R_{FC} = 5.0 \pm 0.2\%$. Combining our measurement of R_{FC} with the sum condition $FC_{000-000} + FC_{100-000} \leqslant 1$, we obtain the following value for the off-diagonal factor $FC_{100-000} = \left(4.8 \pm 0.2_{stat} \pm 0.8_{syst}\right) \times 10^{-2}$. The systematic error contribution is estimated from the laser frequency lock error $\triangle\nu \approx 10$ MHz and using the Doppler lineshape function for the measured linewidth $\triangle\nu_D \approx 40$ MHz. We assume a simple harmonic oscillator model of molecular potentials [44] to estimate $FC_{200-000} \leqslant 1 \times 10^{-3}$. The extracted value of the diagonal factor $FC_{000-000} = (95.2 \pm 0.8) \times 10^{-2}$ together with the sum condition $FC_{000-000} + FC_{000-100} \leqslant 1$ lead to a value for the off-diagonal factor of $FC_{000-100} = \left(4.8^{+0.8}_{-0.9}\right) \times 10^{-2}$. The error in the measured $FC_{000\text{-}100}$ accounts for a possible decay to $\tilde{X}(200)$ with the estimated FC factor of $FC_{000-200} \approx \frac{FC^2_{000-100}}{2FC_{000-000}} \approx 1.2 \times 10^{-3}$ in the harmonic oscillator model [42, 44]. Our result indicates that the SrOH $\tilde{A} - \tilde{X}$ FC array is highly diagonal, and it should be possible to scatter $\sim 10^3$ photons for SrOH using two lasers ($\lambda_{\tilde{A}(000)\leftarrow\tilde{X}(000)}$ and $\lambda_{\tilde{A}(000)\leftarrow\tilde{X}(100)}$) before the molecules will decay to the $\tilde{X}(200)$ state. In order to determine branching ratios to the excited bending vibrations in the $\tilde{X}$ state a more detailed experimental and theoretical analysis is necessary, which is beyond the scope of this paper. By driving $N' = 0 \leftarrow N'' = 1$ transitions, the rotational loss channel can be eliminated [45]. In addition to the possibility of laser cooling, this may also have important applications for sensitive molecule detection in the magnetic trap environment [46].

4. Conclusions

Our measurement of the collisional quenching coefficient γ_{100} and an upper bound on γ_{010} in SrOH–^{4}He collisions provide important information on the interactions between polyatomic molecules and ^{1}S-state atoms at temperatures near 1 K. Below we compare our measurements with other experimental values for diatomics in the similar collisional energy regime (multiple-partial waves):

System	γ	ω, cm^{-1}	T, K
NH–^{3}He [22]	$>5 \times 10^4$	3093	0.6
CaH–^{3}He [25]	$>9 \times 10^5$	1258	0.5
ThO–^{3}He [23]	2×10^4	896	1.2
SrOH(100)–^{4}He	700	527	2.2
SrOH(010)–^{4}He	<100	364	2.2

Since SrOH is a relatively heavy molecule with a large density of rovibrational states it is not surprising that vibrational quenching proceeds relatively quickly. Our results indicate that buffer-gas cooling with helium can efficiently thermalize not only translational and rotational but also vibrational degrees of freedom in polyatomic molecules with low frequency vibrational modes ($\omega < 600$ cm^{-1}) at timescales <1 ms. Study of SrOH–He cold

collisions provides benchmark information on the dependence of vibrational quenching rates on the frequencies of molecular vibrations. The experimental techniques demonstrated in this work can be easily extended to the study of buffer-gas cooling and inelastic collisions for other linear polyatomic molecules (for example CaOH and BaOH). Future work can include experimental investigation of vibrational quenching for different modes in planar (e.g. $SrNH_2$) and symmetric-top (e.g. $SrCH_3$) molecules.

Acknowledgments

We would like to acknowledge Professor TC Steimle who provided us with the measurements of SrOH $\tilde{A}^2\Pi_{1/2}(000) \leftrightarrow \tilde{X}^2\Sigma^+(000)$ transition frequencies. We also would like to thank TV Tscherbul, D Patterson and TC Steimle for insightful discussions. This work was supported by the NSF.

References

[1] Carr L D, DeMille D, Krems R V and Ye J 2009 *New J. Phys.* **11** 055049
[2] Hummon M T, Kłos T V T anJ, Lu H-I, Tsikata E, Campbell W C, Dalgarno A and Doyle J M 2011 *Phys. Rev. Lett.* **106** 053201
[3] Krems R V 2008 *Phys. Chem. Chem. Phys.* **10** 4079
[4] ACME Collaboration 2014 *Science* **343** 269
[5] Hudson J, Kara D, Smallman I, Sauer B, Tarbutt M and Hinds E 2011 *Nature* **473** 493
[6] DeMille D 2002 *Phys. Rev. Lett.* **88** 067901
[7] André A, DeMille D, Doyle J M, Lukin M D, Maxwell S E, Rabl P, Schoelkopf R J and Zoller P 2006 *Nat. Phys.* **2** 636
[8] Micheli A, Brennen G and Zoller P 2006 *Nat. Phys.* **2** 341
[9] Weiner J, Bagnato V S, Zilio S and Julienne P S 1999 *Rev. Mod. Phys.* **71** 1
[10] Sawyer B C, Stuhl B K, Yeo M, Tscherbul T V, Hummon M T, Xia Y, Kłos J, Patterson D, Doyle J M and Ye J 2011 *Phys. Chem. Chem. Phys.* **13** 19059
[11] Stuhl B K, Hummon M T, Yeo M, Quéméner G, Bohn J L and Ye J 2012 *Nature* **396** 492
[12] Kirste M, Wang X, Schewe H C, Meijer G, Liu K, van der Avoird A, Janssen L M, Gubbels K B, Groenenboom G C and van de Meerakker S Y 2012 *Science* **338** 1060
[13] Osterwalder A, Meek S A, Hammer G, Haak H and Meijer G 2010 *Phys. Rev.* A **81** 051401
[14] van de Meerakker S Y, Smeets P H, Vanhaecke N, Jongma R T and Meijer G 2005 *Phys. Rev. Lett.* **94** 023004
[15] Sage J M, Sainis S, Bergeman T and DeMille D 2005 *Phys. Rev. Lett.* **94** 203001
[16] Hudson E R, Gilfoy N B, Kotochigova S, Sage J M and DeMille D 2008 *Phys. Rev. Lett.* **100** 203201
[17] Ni K-K, Ospelkaus S, de Miranda M, Pe'er A, Neyenhuis B, Zirbel J, Kotochigova S, Jin D, Ye J and Julienne P 2008 *Science* **322** 231
[18] Campbell W C, Tscherbul T V, Lu H-I, Tsikata E, Krems R V and Doyle J M 2009 *Phys. Rev. Lett.* **102** 013003
[19] Maussang K, Egorov D, Helton J S, Nguyen S V and Doyle J M 2005 *Phys. Rev. Lett.* **94** 123002
[20] Weinstein J D, deCarvalho R, Guillet T, Friedrich B and Doyle J M 1998 *Nature* **395** 148
[21] Rellergert W G, Sullivan S T, Schowalter S J, Kotochigova S, Chen K and Hudson E R 2013 *Nature* **495** 490
[22] Campbell W C, Groenenboom G C, Lu H-I, Tsikata E and Doyle J M 2008 *Phys. Rev. Lett.* **100** 083003
[23] Au Y S, Connolly C B, Ketterle W and Doyle J M 2014 *Phys. Rev.* A **90** 032703
[24] Piskorski J 2014 *Ph.D Thesis* Harvard University, Cambridge, MA
[25] Weinstein J D 2001 *Ph.D Thesis* Harvard University, Cambridge, MA
[26] Campbell W C and Doyle J M 2009 *Cold Molecules: Theory, Experiment Applications*
[27] Hemmerling B, Drayna G K, Chae E, Ravi A and Doyle J M 2014 *New J. Phys.* **16** 063070
[28] Presunka P I and Coxon J A 1995 *Chem. Phys.* **190** 97
[29] Patterson D and Doyle J M 2007 *J. Chem. Phys.* **126** 154307
[30] Hasted J B 1972 *Physics of Atomic Collisions* (Butterworth& Co)
[31] Li Z, Krems R V and Heller E J 2014 *J. Chem. Phys.* **141** 104317
[32] Lu H-I, Rasmussen J, Wright M J, Patterson D and Doyle J M 2011 *Phys. Chem. Chem. Phys.* **13** 18986
[33] Beardah M S and Ellis A M 1999 *J. Chem. Phys.* **110** 11244
[34] Pereira R and Levy D H 1996 *J. Chem. Phys.* **105** 9733
[35] Skoff S, Hendricks R, Sinclair C, Hudson J, Segal D, Sauer B, Hinds E and Tarbutt M 2011 *Phys. Rev.* A **83** 023418
[36] Hutzler N R, Lu H-I and Doyle J M 2012 *Chem. Rev.* **112** 4803
[37] di Rosa M 2004 *Eur. Phys. J.* D **31** 395
[38] Hunter L, Peck S, Greenspon A, Alam S S and DeMille D 2012 *Phys. Rev.* A **85** 012511
[39] Wall T, Kanem J, Hudson J, Sauer B, Cho D, Boshier M, Hinds E and Tarbutt M 2008 *Phys. Rev.* A **78** 062509
[40] Zhuang X *et al* 2011 *Phys. Chem. Chem. Phys.* **13** 19013
[41] Bernath P F 2005 *Spectra of Atoms and Molecules* (Oxford: Oxford University Press)
[42] Kozyryev I, Baum L, Matsuda K, Olson P, Hemmerling B and Doyle J M 2015 *Supplementary Mater.*
[43] Oberlander M D 1995 *PhD Thesis* Ohio State University
[44] Nicholls R 1981 *J. Astrophys. Suppl. S.* **47** 279
[45] Shuman E S, Barry J F, Glenn D R and DeMille D 2009 *Phys. Rev. Lett.* **103** 223001
[46] Lu H-I, Kozyryev I, Hemmerling B, Piskorski J and Doyle J M 2014 *Phys. Rev. Lett.* **112** 113006